

# Kinetics of Soluble Chromium Removal from Contaminated Water by Zerovalent Iron Media: Corrosion Inhibition and Passive Oxide Effects

NIKOS MELITAS,  
OUATFA CHUFFE-MOSCOSO, AND  
JAMES FARRELL\*

Department of Chemical and Environmental Engineering,  
University of Arizona, Tucson, Arizona 85721

Permeable reactive barriers containing zerovalent iron are being increasingly employed for in situ remediation of groundwater contaminated with redox active metals and chlorinated organic compounds. This research investigated the effect of chromate concentration on its removal from solution by zerovalent iron. Removal rates of aqueous Cr(VI) by iron wires were measured in batch experiments for initial chromium concentrations ranging from 100 to 10 000  $\mu\text{g/L}$ . Chromate removal was also measured in columns packed with zerovalent iron filings over this same concentration range. Electrochemical measurements were made to determine the free corrosion potential and corrosion rate of the iron reactants. In both the batch and column reactors, absolute rates of chromium removal declined with increasing chromate concentration. Corrosion current measurements indicated that the rate of iron corrosion decreased with increasing Cr(VI) concentrations between 0 and 5000  $\mu\text{g/L}$ . At a Cr(VI) concentration of 10 000  $\mu\text{g/L}$ , Tafel polarization diagrams showed that chromium removal was affected by its diffusion rate through a passivating oxide film and by the ability of iron to release  $\text{Fe}^{2+}$  at anodic sites. In contrast, water reduction was not mass transfer limited, but chromium did decrease the exchange current for the hydrogen evolution reaction. Even at the most passivating concentration of 10 000  $\mu\text{g/L}$ , effluent Cr(VI) concentrations in the column reactors reached a steady state, indicating that passivation had also reached a steady state. Although chromate contributes to iron surface passivation, the removal rates are still sufficiently fast for in situ iron barriers to be effective for Cr(VI) removal at most environmentally relevant concentrations.

## Introduction

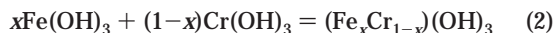
Chromium is one of the most common groundwater contaminants at industrial sites and military facilities due to its widespread use as a metal corrosion inhibitor (1). In recent years, there has been great interest in using permeable reactive barriers containing zerovalent iron for in situ treatment of groundwater contaminated with chlorinated organic compounds and redox active metals (2). For remediating redox active metals, the iron serves as an electron

donor to reduce dissolved metal ions to valence states that are less water soluble. To date, more than 32 permeable barriers have been installed for groundwater remediation in the United States and Canada (3).

Previous investigators have shown that highly water soluble Cr(VI) may be removed from solution via reduction to Cr(III) according to (4–9):



In addition to precipitation of  $\text{Cr(OH)}_3(\text{s})$ , Cr(III) may also form  $\text{Cr}_2\text{O}_3(\text{s})$  or solid solutions with Fe(III) according to (4, 5, 7)



where  $x$  can range from 0 to 1. In addition to reduction by zerovalent iron, Cr(VI) may also be reduced by atomic hydrogen adsorbed to iron surfaces (4, 10, 11), by Fe(II) in solution (11–16), or in mineral phases (17–21), or by dissolved organic compounds (22, 23).

Soluble chromate removal by zerovalent iron media has been described by a kinetic expression of the form (11)

$$\frac{d\{\text{Cr(VI)}\}}{dt} = -kA\{\text{Cr(VI)}\}^{0.5}\{\text{H}^+\}^{0.5} \quad (3)$$

where  $\{\text{Cr(VI)}\}$  is the aqueous chromate activity,  $k$  is the reaction rate constant, and  $A$  is the reactive surface area. The rate constant defined by eq 3 was found to depend on both the solution ionic strength and the mixing rate. Other investigators have found that chromate removal by iron media is dependent on the composition of the iron (5) and may also be affected by the presence of inorganic mineral phases that impact the solution chemistry (4).

The kinetic expression in eq 3 is 0.5 order in Cr(VI) concentration. Reaction orders less than unity are often indicative of reactive site saturation effects. However, in the case of zerovalent iron, the number and activity of the reactive sites is not fixed and depends on both the iron and solution potentials. Therefore, the apparent 0.5 reaction order may be due to a rate-limiting mechanism that involves electron transfer and will thus be dependent on both the reactant concentration and the potential of iron.

The effect of potential and Cr(VI) concentration on the chromate reduction current ( $I$ ) associated with a corroding iron electrode can be described by (24)

$$I = nFAk\{\{\text{Cr(VI)}\}e^{-\beta_c^{\text{Cr}}(E_{\text{corr}} - E^0)} - \{\text{Cr(III)}\}e^{\beta_a^{\text{Cr}}(E_{\text{corr}} - E^0)}\} \quad (4)$$

where  $n$  is the number of electrons transferred;  $F$  is the Faraday constant;  $A$  is the reactive surface area;  $k$  is the standard rate constant;  $\beta_c^{\text{Cr}}$  and  $\beta_a^{\text{Cr}}$  are the cathodic and anodic Tafel slopes, respectively, for the Cr(VI)/Cr(III) redox couple;  $E^0$  is the standard reduction potential for the Cr(VI)/Cr(III) redox couple;  $E_{\text{corr}}$  is the free corrosion potential; and  $\{\text{Cr(VI)}\}$  and  $\{\text{Cr(III)}\}$  are the activities of the Cr(VI) and Cr(III) species, respectively. The standard rate constant is independent of potential and depends only on the kinetic facility of the redox reaction on the surface of interest (24).

Field studies have demonstrated that permeable iron barriers are effective for Cr(VI) removal over extended periods of operation (25–27). However, chromate is a strong oxidant and is a well-known passivator of iron (10). Therefore, the buildup of chromium compounds on the iron surfaces may

\* Corresponding author phone: (520)621-2465; fax: (520)621-6048; e-mail: farrell@engr.arizona.edu.

decrease reaction rates for chromate removal. This research investigated the hypothesis that increasing concentrations of chromate may contribute to decreasing reaction rates through increased surface passivation. The specific objectives of this investigation were to determine the effect of the Cr(VI) concentration on its removal rate and on the corrosion rate of the zerovalent iron.

## Materials and Methods

**Batch Reactors.** Batch experiments measuring soluble Cr(VI) removal by iron wires were performed in well-stirred, sealed 0.85 L glass reactors containing potassium chromate in 3 mM CaSO<sub>4</sub> background electrolyte solutions. In experiments measuring Cr(VI) removal rates, a single 10 cm long by 1.2 mm diameter iron wire of 99.9% purity (Aesar, Ward Hill, MA) was used as the reactant. Anaerobic conditions were maintained by purging the reactors with humidified nitrogen gas. Samples were taken using a 1 mL glass syringe, with and without 0.1  $\mu$ m nylon syringe filters (Whatman, Clifton, NJ). In all experiments, solution pH values were measured with color-calibrated test strips, and aqueous chromium concentrations were determined using a Perkin-Elmer (San Jose, CA) model 4110zL graphite furnace atomic absorption spectrophotometer.

**Packed Column Experiments.** Column experiments were performed using either a 50 cm long by 2.5 cm outer diameter (o.d.) glass column or a 25 cm long by 0.9 cm o.d. stainless steel column. Both columns were packed with Master Builder's Supply (Cleveland, OH) iron filings GX-27 blend. The glass column contained three intracolumn sampling ports at 12.5, 25, and 37.5 cm from the influent end. One port at each location served for taking aqueous samples and for measuring the redox potential of the solution. The other port was used to determine the free corrosion potential of the iron reactants. The corrosion potentials were measured using an iron wire permanently inserted into the column through a rubber septum at each port. The columns were operated with Cr(VI) concentrations ranging from 100 to 10 000  $\mu$ g/L in 3 mM CaSO<sub>4</sub> background electrolyte solutions. The mean hydraulic residence time in the 25 cm column was 25 min and was 19 min in the 50 cm column.

**Electrochemical Experiments.** Two types of electrochemical experiments were performed to assess the effect of chromate concentration on iron corrosion rates. To assess the effect of concentration on initial rates of iron corrosion, a single 10 cm long iron wire was placed in 0.75 L of 3 mM CaSO<sub>4</sub> electrolyte solution in one of the glass reactors containing a calomel reference electrode and a stainless steel counter electrode. The solution was continuously purged with 50 mL/min of humidified nitrogen gas, and potassium chromate was added to the reactor through the vent tubing to produce dissolved chromium concentrations ranging from 100 to 10 000  $\mu$ g/L. The wire was exposed to each concentration for 1 day, at which point a Tafel scan was performed.

To determine the effect of elapsed time on iron corrosion rates in solutions of approximately constant chromium concentration, 2.6 cm long iron wires were placed in the nitrogen-purged, glass reactors containing Cr(VI) at concentrations of 0, 100, 5000, or 10 000  $\mu$ g/L. Short wires were used in order to minimize changes in solution concentration over the course of these experiments. Tafel scans were performed to measure changes in the corrosion currents and free corrosion potentials as a function of elapsed time.

All Tafel diagrams were produced by polarizing the wires  $\pm 200$  mV with respect to their open circuit potentials (28). The polarization experiments were performed using an EG&G (Oak Ridge, TN) model 273A scanning potentiostat and M270 software. All potentials are reported with respect to the standard hydrogen electrode (SHE).

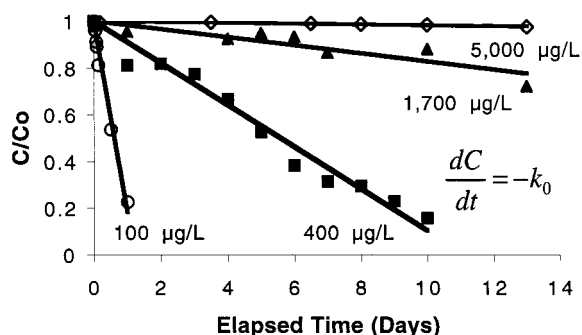


FIGURE 1. Aqueous Cr(VI) concentrations in the iron wire batch reactors with differing initial Cr(VI) concentrations. Zero order ( $k_0$ ) removal rate constants for each initial concentration are presented in Table 1.

TABLE 1. Zero Order Rate Constants ( $k_0$ ) with 95% Confidence Intervals for Chromate Removal from Solutions with Different Initial Cr(VI) Concentrations ( $C_0$ )

$C_0$ ( $\mu$ g/L)	$k_0$ ( $\mu$ g/m <sup>2</sup> min)	correlation coeff ( $R^2$ )
100	$94 \pm 10$	0.98
400	$56 \pm 7$	0.97
1700	$48 \pm 22$	0.82
5000	$14 \pm 7$	0.86

## Results and Discussion

**Removal Kinetics.** Aqueous chromate concentrations in the batch reactors as a function of elapsed time are shown in Figure 1. Filtered and unfiltered samples gave similar results, indicating that the chromate removed from solution was associated with the iron wires. Comparison of chromium removal rates in stirred and unstirred reactors indicated that the observed rates were not significantly affected by hydrodynamic boundary layer mass transfer limitations. In all experiments, pH values remained constant at approximately 7. No detectable removal was observed in the reactor with an initial concentration of 10 000  $\mu$ g/L. In the remaining reactors, the chromate removal kinetics could be adequately described by a zero-order kinetic model, as illustrated in Figure 1. However, for initial concentrations between 100 and 5000  $\mu$ g/L, the observed removal rates decreased with increasing chromate concentration, as shown in Table 1.

The decreasing Cr(VI) removal rates with increasing concentration can be explained by lower rates of iron corrosion at higher chromate concentrations. Figure 2a shows the corrosion rate of a single iron wire exposed to increasing chromate concentrations for 1 day at each concentration. The higher corrosion potentials and lower corrosion currents observed with increasing concentration between 100 and 5000  $\mu$ g/L are indicative of the action of an oxidant/passivator like chromate (28, 29). As shown in Figure 2b, corrosion currents in the constant concentration reactors also decreased with increasing chromate concentration.

In contrast to many catalytic systems where the activity of the reactive sites is independent of the reactant concentration, the reactivity of sites on zerovalent iron may be expected to decline with increasing oxidant concentration. This can be attributed to the effect of potential on the rate of electrochemical reactions and on the passivating effect of a corrosion inhibitor like chromate. As shown by the potential data in Figure 2a, between 100 and 5000  $\mu$ g/L, higher Cr(VI) concentrations resulted in higher  $E_{\text{corr}}$  values. According to eq 4, the rate of Cr(VI) reduction by zerovalent iron should be dependent on both the Cr(VI) concentration and the potential of the iron. However, the behavior predicted by eq 4 is not consistent with the results in Table 1. For example,

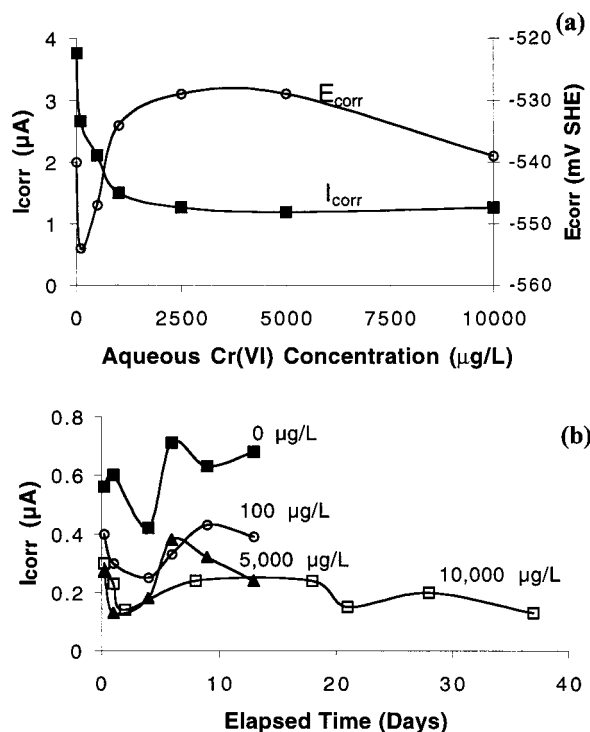


FIGURE 2. (a) Corrosion currents ( $I_{\text{corr}}$ ) and free corrosion potentials ( $E_{\text{corr}}$ ) for a single 10 cm long iron wire immersed in anaerobic Cr(VI) solutions after 1 day elapsed at each concentration. The wire was exposed to each Cr(VI) concentration for 1 day before each measurement was taken. (b) Corrosion currents for 2.6 cm long iron wires immersed in anaerobic solutions of different initial Cr(VI) concentration. In the 5000 and 10 000  $\mu\text{g/L}$  reactors, there was no measurable Cr(VI) removal over the duration of the current measurements.

using the measured cathodic Tafel slope for Cr(VI) reduction of 0.0049 dec/mV and the potential data in Figure 2a, eq 4 predicts that the Cr(VI) removal rate at a concentration of 5000  $\mu\text{g/L}$  should be 44 times greater than that observed at a concentration of 100  $\mu\text{g/L}$ . However, as shown in Table 1, the removal rate actually declined with increasing Cr(VI) concentration. This behavior can only be attributed to increasing iron surface passivation with increasing chromate concentration.

Iron surface passivation can be attributed to both anodic and cathodic inhibition of iron corrosion. The cathodic ( $I_c$ ) and anodic ( $I_a$ ) currents produced in the Tafel scans can be expressed as (28)

$$I_c = I_0^c e^{-\beta_c(E - E_{\text{eq}}^c)} \quad (5)$$

$$I_a = I_0^a e^{\beta_a(E - E_{\text{eq}}^a)} \quad (6)$$

where  $I_0^a$  and  $I_0^c$  are the anodic and cathodic exchange currents, respectively, while  $E_{\text{eq}}^a$  and  $E_{\text{eq}}^c$  are the equilibrium potentials for the anodic and cathodic redox reactions. The exchange currents depend on the kinetic facility of the reaction, the reactant concentrations, and the surface area available for reduction or oxidation (28). Figure 3a compares Tafel diagrams generated in the blank and 100  $\mu\text{g/L}$  solutions. The cathodic Tafel slopes of 0.0065 dec/mV in both solutions are similar to literature values for water reduction in neutral and alkaline media of 0.006 to 0.0072 dec/mV (30–32). This indicates that water was the primary oxidant in both solutions and that the current associated with Cr(VI) reduction was too low to measurably contribute to the observed corrosion current.

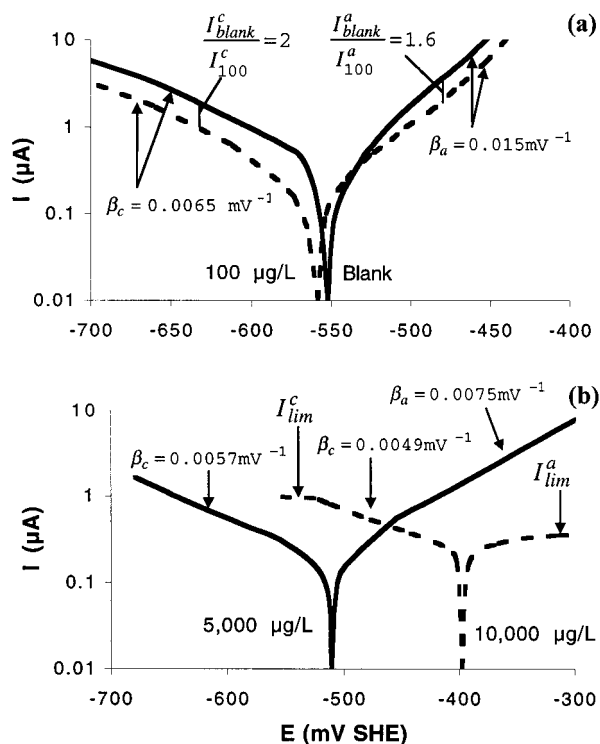


FIGURE 3. Tafel scans after 1 day elapsed for 2.6 cm long iron wires immersed in anaerobic 3 mM  $\text{CaSO}_4$  background electrolyte solutions with initial Cr(VI) concentrations of (a) 0 and 100  $\mu\text{g/L}$  and (b) 5000 and 10 000  $\mu\text{g/L}$ .

Although the Tafel slopes shown in Figure 3a were similar in both solutions, there was lower current at each potential in the Cr(VI) containing reactor. As illustrated by eq 5, the lower cathodic current in the chromate reactor can be attributed to a factor of 2 decline in  $I_0^c$  for water reduction. This decrease in  $I_0^c$  for water can likely be attributed to the deposition of Cr(III) oxides at cathodic sites on the iron surface (32, 33). Spectroscopic analysis has found that both  $\text{Cr}(\text{OH})_3$  and  $\text{Cr}_2\text{O}_3$  deposit at cathodic sites on iron surfaces (7, 9, 32). As illustrated by eq 6, the lower anodic current in the chromate versus the blank solution can be attributed to a decrease in  $I_0^a$ . This factor of 1.6 decline in current in the anodic Tafel region likely results from the presence of Fe(III) or mixed Cr(III)/Fe(III) oxides at anodic sites on the iron surface. These oxides decrease the surface area available for the anodic reaction of iron oxidation.

Figure 3b shows Tafel scans taken after 1 day elapsed for the iron wires immersed in the 5000 and 10 000  $\mu\text{g/L}$  Cr(VI) solutions. Comparison of the diagrams in Figure 3a,b show that the  $\beta_c$  values after 1 day elapsed decreased with increasing Cr(VI) concentration. This can be attributed to a decreasing contribution of water reduction to the total rate of iron corrosion. The inhibition of water reduction was caused by the increase in potential of the iron and by a decrease in the  $I_0^c$  for water reduction. At a chromate concentration of 100  $\mu\text{g/L}$ , the  $\beta_c$  of 0.0065 dec/mV indicates that water reduction was the primary cathodic reaction. However, inhibition of water reduction increased the contribution of other cathodic reactions to the observed corrosion current. At a concentration of 10 000  $\mu\text{g/L}$ , reduction of chromate appears to be the dominant reaction contributing to iron corrosion after 1 day elapsed. The  $\beta_c$  of 0.0049 dec/mV in the 10 000  $\mu\text{g/L}$  solution is close to the  $\beta_c$  of 0.0050 dec/mV observed by other investigators for a chromate-coated iron electrode immersed in a 780 000  $\mu\text{g/L}$  Cr(VI) solution (32). Additionally, the potential in the 10 000  $\mu\text{g/L}$  solution of -400 mV is close to the equilibrium potential for water reduction, indicating that



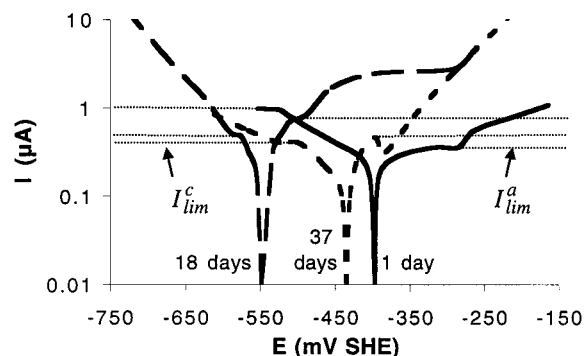


FIGURE 4. Tafel scans after 1, 18, and 37 days elapsed for a 2.6 cm long iron wire electrode immersed in an anaerobic 3 mM  $\text{CaSO}_4$  background electrolyte solution with an initial  $\text{Cr(VI)}$  concentration of 10 000  $\mu\text{g/L}$ .

there was minimal hydrogen evolution after 1 day elapsed. As shown in Figure 3b, the  $\beta_c$  of 0.0057 dec/mV in the 5000  $\mu\text{g/L}$  solution was intermediate to the  $\beta_c$  values in the blank and 10 000  $\mu\text{g/L}$  reactors. This indicates that both water and chromate reduction contributed to the observed rate of iron corrosion at 5000  $\mu\text{g/L}$ .

Mass transfer limitations are evident in the cathodic Tafel slopes in the 10 000  $\mu\text{g/L}$  solution. The flattening of the 10 000  $\mu\text{g/L}$  cathodic Tafel slope in Figure 3b at a current of 1  $\mu\text{A}$  was due to mass transfer effects. During the cathodic scan, reduction of  $\text{Cr(VI)}$  decreased the chromate concentration in the vicinity of the cathodic sites. At a potential of -520 mV, the rate of reduction became faster than the rate of  $\text{Cr(VI)}$  diffusion to cathodic sites. This limited the reduction rate to the rate of chromate diffusion and resulted in a cathodic mass transfer limited current ( $I_{\text{lim}}^c$ ) of  $\sim 1 \mu\text{A}$ .

There was a gradual decline in  $I_{\text{lim}}^c$  at 10 000  $\mu\text{g/L}$  with increasing elapsed time. Tafel scans for this reactor at 1, 18, and 37 days elapsed are compared in Figure 4. The  $I_{\text{lim}}^c$  values for  $\text{Cr(VI)}$  reduction declined from  $\sim 1 \mu\text{A}$  after 1 day elapsed to 0.4  $\mu\text{A}$  after 37 days. This can be attributed to increasing mass transfer limitations for  $\text{Cr(VI)}$  reduction with elapsed time. However, the small difference in mass transfer limitations between 18 and 37 days suggests that the surface passivation was approaching a steady state.

The  $\text{Cr(VI)}$  concentration also affected the anodic Tafel slopes in each reactor. As illustrated by the  $\beta_a$  values in Figure 3a,b, increasing chromate concentrations resulted in decreasing anodic Tafel slopes for iron oxidation. Decreasing  $\beta_a$  values are indicative of increasing anodic inhibition of iron corrosion. This inhibition likely arises from formation of  $\text{Fe(III)}$  and  $\text{Fe(III)/Cr(III)}$  oxides produced via reaction of  $\text{Cr(VI)}$  with  $\text{Fe}^{2+}$  released at anodic sites (4, 10). These insoluble oxides decrease the rate that  $\text{Fe}^{2+}$  released at underlying anodic sites may enter the solution. The buildup of  $\text{Fe}^{2+}$  under the oxide layer leads to concentration polarization and thereby reduces the thermodynamic favorability for further iron oxidation. This effect is essentially a mass transfer limitation on the iron oxidation reaction.

Although increasing cathodic inhibition was observed with elapsed time in Figure 4, there was decreasing anodic inhibition between 1 and 18 days elapsed. This decreasing anodic inhibition can be seen by the greater mass transfer limited current for iron oxidation ( $I_{\text{lim}}^a$ ) at 18 days compared to that at 1 day. This type of behavior has been attributed to reductive dissolution of the iron oxide film, and to morphological changes in the oxides coating the iron (34). Changing oxide morphology can be seen in the Tafel slopes that occur after the mass transfer limited current for iron oxidation. The 1 and 18 day scans in Figure 4 show two additional anodic Tafel slopes, while the 37 day scan shows

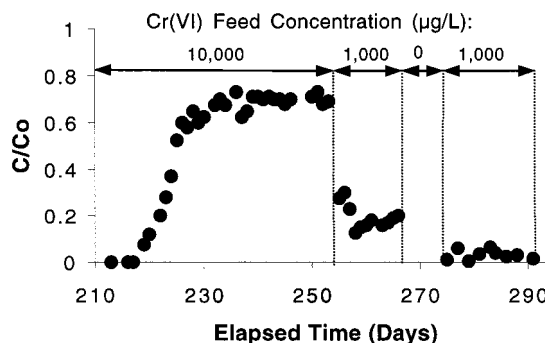


FIGURE 5. Effluent chromium concentrations as a function of elapsed time for a 25 cm long column packed with 40 g of iron filings and operated at  $\text{Cr(VI)}$  concentrations ranging from 100 to 10 000  $\mu\text{g/L}$  in an anaerobic 3 mM  $\text{CaSO}_4$  background electrolyte solution. Influent and effluent chromium concentrations for the entire experiment are listed in Table 2.

TABLE 2. Influent and Effluent  $\text{Cr(VI)}$  Concentrations for the 25 cm Column Operated with a Mean Hydraulic Detention Time of 25 min

days elapsed	influent concn ( $\mu\text{g/L}$ )	effluent concn ( $\mu\text{g/L}$ )
0–117	100	0
117–132	300	0
132–146	600	0
146–183	1000	0
183–193	1500	0
193–207	5000	0
207–252	10 000	7000
252–267	1000	200
267–274	shut-in	shut-in
274–296	1000	20

only one additional slope beyond that for iron oxidation. These additional slopes result from oxidation of different iron oxides (32). The fact that there was only one oxide Tafel slope at 37 days elapsed suggests that the oxide is more uniform at this time than at 1 and 18 days.

Changes in the oxide coating the iron are reflected in changes in electrode potential. The temporal oscillations in  $E_{\text{corr}}$  illustrated for the 10 000  $\mu\text{g/L}$  reactor in Figure 4 were observed in all reactors. These potential oscillations are associated with oscillations in  $\text{Cr(VI)}$  removal rates, as illustrated in Figure 1 for the 400 and 1700  $\mu\text{g/L}$  reactors. Periods of declining potential are associated with faster removal rates, while periods of increasing potential are associated with slower removal rates.

**Column Results.** Results from a long-term column experiment measuring  $\text{Cr(VI)}$  removal rates as a function of influent concentration are shown in Figure 5. The influent  $\text{Cr(VI)}$  concentration for each period are summarized in Table 2. Influent and effluent pH values were always  $7 \pm 0.5$ . For influent  $\text{Cr(VI)}$  concentrations between 100 and 5000  $\mu\text{g/L}$ , effluent concentration in the 25 cm column remained below the detection limit of 0.5  $\mu\text{g/L}$ . This indicates that rates of  $\text{Cr(VI)}$  removal were too fast to be measured for influent concentrations between 100 and 5000  $\mu\text{g/L}$ . However, as shown in Figure 5, an influent concentration of 10 000  $\mu\text{g/L}$  resulted in chromium breakthrough, with a steady-state effluent concentration of  $\sim 7000 \mu\text{g/L}$ . This steady-state removal was observed for a period of 30 days ( $\sim 1700$  pore volumes) until the experimental conditions were changed.

Upon lowering the influent concentration back to 1000  $\mu\text{g/L}$  at 252 days elapsed, the effluent concentration declined to a steady-state value of  $\sim 200 \mu\text{g/L}$ . Previously, as shown in Table 2, an influent concentration of 1000  $\mu\text{g/L}$  resulted

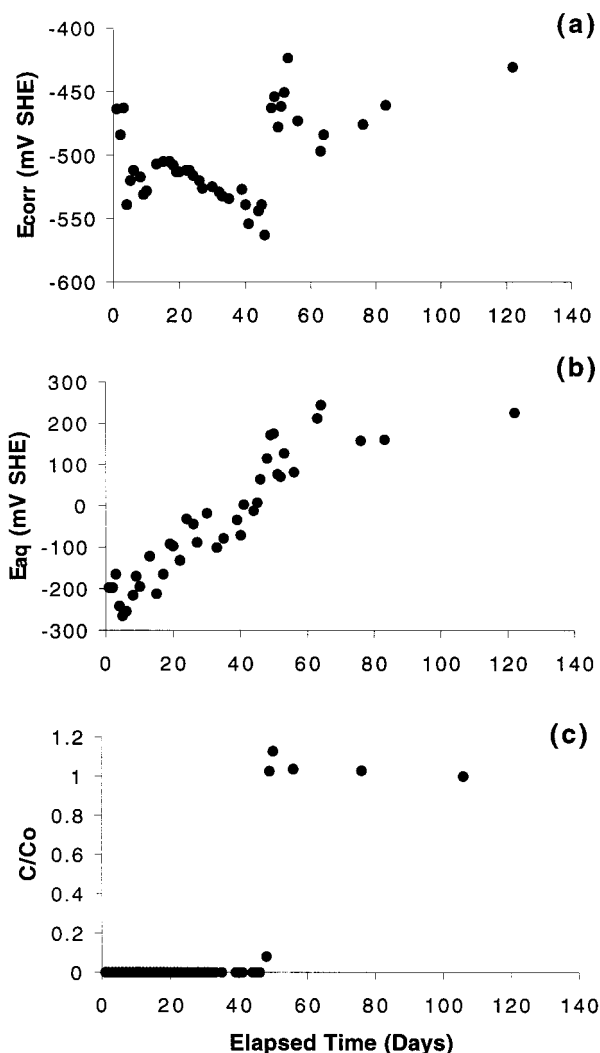


FIGURE 6. Data for a 50 cm long column packed with 323 g of iron filings and operated with influent Cr(VI) concentrations ranging from 100 to 10 000  $\mu\text{g/L}$  in an anaerobic 3 mM  $\text{CaSO}_4$  background electrolyte solution. Influent and effluent chromium concentrations for the entire experiment are listed in Table 3: (a)  $E_{corr}$  values for an iron wire probe permanently inserted into the column at the middle sampling port; (b) solution potentials measured at the middle sampling port; and (c) aqueous chromium concentrations at the middle sampling port.

in complete chromium removal. Therefore, the greater effluent concentration between 252 and 267 days indicates that exposure of the iron to the 10 000  $\mu\text{g/L}$  solution produced a loss in reactivity that resulted in slower rates of Cr(VI) removal. However, this loss in reactivity was slowly reversible. To investigate recovery in iron reactivity, the column was sealed between 267 and 274 days elapsed. Upon resuming flow at an influent concentration of 1000  $\mu\text{g/L}$ , the effluent concentration decreased to  $\sim 20 \mu\text{g/L}$ , as shown in Figure 5. This behavior indicates that the performance of zerovalent iron for Cr(VI) removal is hysteretic and is highly dependent on the condition of the iron surfaces.

Data from the 50 cm glass column indicate that the condition of the iron surfaces varied with time and location along the length of the column. In all three sampling ports, the potential of the iron decreased with elapsed time until the chromate front reached that port. Figure 6a shows the iron wire potential from the middle sampling port of the glass column, while Figure 6b,c show the solution potential ( $E_{aq}$ ) and chromate concentration, respectively. During the period when there was complete chromate removal before

TABLE 3. Influent and Effluent Cr(VI) Concentrations for the 50 cm Column Operated with a Mean Hydraulic Detention Time of 19 min

days elapsed	influent concn ( $\mu\text{g/L}$ )	effluent concn ( $\mu\text{g/L}$ )
0–6	100	0
6–12	200	0
12–18	400	0
18–24	800	0
24–32	1200	0
32–40	2500	0
40–46	5000	0 <sup>a</sup>
46–122	10 000	9100

<sup>a</sup> Steady-state concentration of 580  $\mu\text{g/L}$  was observed at port 1.

sampling port 2, a continuous decrease in  $E_{corr}$  was observed after an initial potential fluctuation. This decreasing potential is consistent with the potential behavior in the batch experiments and cannot be explained by changes in solution potential, since the solution potential increased monotonically with time. The potential fluctuations observed during the first 15 days elapsed can most likely be attributed to reduction of the air-formed oxide and the subsequent formation of  $\text{Fe}(\text{OH})_2$  (35). The almost linear potential drop between 15 and 47 days elapsed can likely be attributed to transformation of  $\text{Fe}(\text{OH})_2$  to a porous layer of magnetite ( $\text{Fe}_3\text{O}_4$ ), as observed by previous investigators (35).

Upon breakthrough, and exposure of the iron wire in the center port to chromate at 47 days elapsed, the potential sharply increased due to the oxidizing action of chromate and the formation of passivating Fe(III)/Cr(III) oxides. The subsequent potential decline between 55 and 63 days elapsed can likely be attributed to reduction of the passive film (34). After 63 days elapsed, the potential gradually increased due to continuous exposure to high Cr(VI) concentrations and the build-up of a chromium-enforced passive layer. Similar temporal oscillations in potential were observed for all three intracolumn iron wire probes, and in the batch experiments, as illustrated in Figure 4 for the 10 000  $\mu\text{g/L}$  reactor.

Overall Cr(VI) removal in the 50 cm glass column was similar to that observed in the 25 cm column. As indicated in Table 3, feed concentrations less than 5000  $\mu\text{g/L}$  resulted in complete chromium removal before the first sampling port, and the first appearance of measurable chromium in the column effluent occurred at a feed concentration of 10 000  $\mu\text{g/L}$ . Since measurable chromium concentrations were observed only for the two highest feed concentrations, Cr(VI) removal rates can be calculated only for influent concentrations of 5000 and 10 000  $\mu\text{g/L}$ . Mass balances on the column showed steady-state removal rates of 707 and 36  $\mu\text{g}/(\text{L min})$  for influent concentrations of 5000  $\mu\text{g/L}$  and 10 000  $\mu\text{g/L}$ , respectively. This decrease in removal rate with increased feed concentration is consistent with results of the batch tests and illustrates that Cr(VI) removal kinetics cannot be described by simple zero, first, or fractional order kinetic models that do not account for iron surface passivation.

Even at the most passivating concentration of 10 000  $\mu\text{g/L}$ , effluent chromate concentrations in both columns reached a steady state within several days. This indicates that the extent of surface passivation had also reached a steady state. Steady state performance may be attributed to continuous generation of new diffusion pathways and reaction sites arising from crack formation in the oxide layer. This is consistent with previous reports that only thin passive films may remain nonporous, since internal stresses lead to crack formation as the oxide film grows (36, 37).

Similar cathodic and anodic mass transfer limited currents at 37 days elapsed in the 10 000  $\mu\text{g/L}$  solution indicate that

chromium removal rates are affected by both the ability of Cr(VI) to penetrate passivating oxides and by the ability of iron to release  $\text{Fe}^{2+}$  at anodic sites. Although Cr(VI) concentrations as low as 100  $\mu\text{g/L}$  significantly decrease corrosion rates, concentration increases above 1000  $\mu\text{g/L}$  have only a minimal effect on the rate of corrosion, despite significantly impacting the rate of Cr(VI) removal. This is consistent with an oxide film that acts as a diffusion barrier for Cr(VI) reduction. Since rates of Cr(VI) removal are limited by its mass transfer and the mass transfer of  $\text{Fe}^{2+}$  ions through the oxide film, thicker films associated with higher Cr(VI) concentrations decrease the mass transfer rates and thereby decrease chromate removal rates. In contrast, the Tafel scans indicate water reduction is not limited by mass transfer, and the effect of chromium on hydrogen evolution occurs via directly blocking cathodic sites. Therefore, the thickness of the oxide film has only a small impact on the rate of water reduction.

Although results from this research show that chromate contributes to iron surface passivation, the column results suggest that removal rates can reach steady state values that are sufficiently fast to provide effective removal for most environmentally relevant concentrations, which are often less than 10 000  $\mu\text{g/L}$  (3). This is confirmed by field studies showing that permeable barriers containing zerovalent iron can reduce aqueous Cr(VI) concentrations to nondetectable levels (25–27). For example, a permeable barrier operating at a flow velocity of ~50 cm per day has been effective for treating groundwater with Cr(VI) concentrations up to 10 000  $\mu\text{g/L}$  for more than 2 years (38, 39). This indicates that for typical groundwater flow rates, diffusion of Cr(VI) and  $\text{Fe}^{2+}$  through the passivating films are sufficiently fast to provide for complete Cr(VI) removal. However, since chromate decreases iron corrosion rates, the presence of even low levels of Cr(VI) may adversely affect treatment of other contaminants at sites where permeable barriers are used for remediating plumes containing both chromate and chlorinated organic compounds.

## Acknowledgments

The authors thank Dr. Wayne Seames and Gina Bailey for their assistance. Although the research described in this article has been funded by the United States Environmental Protection Agency through grant R-825223-01-0 to J.F., it has not been subjected to the Agency's peer and policy review and therefore does not necessarily reflect the views of the Agency, and no official endorsement should be inferred.

## Literature Cited

- (1) Kavanaugh, M. C. *Alternatives for Groundwater Cleanup*; National Academy Press: Washington, DC, 1994; 315.
- (2) Gillham, R. W.; O'Hannesin, S. F. *Groundwater* **1994**, 32, 958.
- (3) U.S. EPA. *Field Applications of In Situ Remediation Technologies: Permeable Reactive Barriers*; EPA 542-R-99-002; 1999.
- (4) Powell, R. M.; Puls, W. P.; Hightower, S. K.; Sabatini, D. A. *Environ. Sci. Technol.* **1995**, 29, 1913.
- (5) Astrup, T.; Stipp, S. L. S.; Christensen, T. H. *Environ. Sci. Technol.* **2000**, 34, 4163.
- (6) Mayne, J. E. O.; Pryor, M. J. *J. Chem. Soc.* **1949**, 1831.
- (7) Gould, J. P. *Water Res.* **1982**, 16, 871.
- (8) Buerge, I. J.; Hug, S. J. *Environ. Sci. Technol.* **1998**, 32, 2092.
- (9) Anderson, L. D.; Kent, D. B.; Davis, J. A. *Environ. Sci. Technol.* **1994**, 28, 178.
- (10) Loya-Lawniczak, S.; Refait, P.; Ehrhardt, J. J.; Lecomte, P.; Genin, J. M. R. *Environ. Sci. Technol.* **2000**, 34, 438.
- (11) Deng, B.; Stone, A. T. *Environ. Sci. Technol.* **1996**, 30, 2484.
- (12) Jardine, P. M.; Fendorf, S. E.; Mayes, M. A.; Larsen, S. C.; Brooks, S. C.; Bailey, W. B. *Environ. Sci. Technol.* **1999**, 33, 2939.
- (13) Bard, A. J.; Faulkner, L. R. *Electrochemical Methods*; John Wiley: New York, 1980.
- (14) Blowes, D. W.; Gillham, R. W.; Ptacek, C. J.; Puls, R. W.; Bennett, T. A.; O'Hannesin, S. F.; Hanton-Fong, C. J.; Bain, J. G. *An in situ permeable reactive barrier for the treatment of hexavalent chromium and trichloroethylene in groundwater: Volume 1, Design and installation*; EPA/600/R-99/09; Environmental Protection Agency.
- (15) Puls, R. W.; Paul, C. J.; Powell, R. M. *Appl. Geochem.* **1999**, 14, 989.
- (16) Bockris, J. O'M.; Reddy, A. K. N. *Modern Electrochemistry*; Plenum Press: New York, 1970.
- (17) Uhlig, H. H.; Revie, R. W. *Corrosion and Corrosion Control*, 3rd ed.; John Wiley: New York, 1985.
- (18) Brown, A. P.; Krumpelt, R. O.; Yao, N. P. *J. Electrochem. Soc.* **1982**, 129(11), 2481.
- (19) Cornell, A.; Lindbergh, G.; Simonsson, D. *Electrochim. Acta* **1992**, 37(10), 1873.
- (20) Lindbergh, G.; Simonsson, D. *Electrochim. Acta* **1991**, 36(13), 1985.
- (21) Bonin, P. M. L.; Odziemkowski, M. S.; Gillham, R. W. *Corros. Sci.* **1998**, 40, 1391.
- (22) Odziemkowski, M. S.; Schuhmacher, T. T.; Gillham, R. W.; Reardon, E. J. *Corros. Sci.* **1998**, 40, 371.
- (23) Reardon, E. J. *Environ. Sci. Technol.* **1995**, 29, 2936.
- (24) Balko, B.; Tratnyek, P. G. *J. Phys. Chem. B* **1998**, 102, 1459.
- (25) Puls, R. W.; Blowes, D. W.; Gillham, R. W. *J. Hazard. Mater.* **1999**, 68, 109.
- (26) Blowes, D. W.; Ptacek, C. J.; Benner, S. G.; McRae, C. W. T.; Bennett, T. A.; Puls, R. W. *J. Contaminant Hydrol.* **2000**, 45, 123.
- (27) Puls, R. W.; Paul, C. J.; Powell, R. M. *Appl. Geochem.* **1999**, 14, 989.
- (28) Bockris, J. O'M.; Reddy, A. K. N. *Modern Electrochemistry*; Plenum Press: New York, 1970.
- (29) Uhlig, H. H.; Revie, R. W. *Corrosion and Corrosion Control*, 3rd ed.; John Wiley: New York, 1985.
- (30) Brown, A. P.; Krumpelt, R. O.; Yao, N. P. *J. Electrochem. Soc.* **1982**, 129(11), 2481.
- (31) Kreysa, G.; Hakansson, B. J. *Electroanal. Chem.* **1986**, 201, 61.
- (32) Cornell, A.; Lindbergh, G.; Simonsson, D. *Electrochim. Acta* **1992**, 37(10), 1873.
- (33) Lindbergh, G.; Simonsson, D. *Electrochim. Acta* **1991**, 36(13), 1985.
- (34) Bonin, P. M. L.; Odziemkowski, M. S.; Gillham, R. W. *Corros. Sci.* **1998**, 40, 1391.
- (35) Odziemkowski, M. S.; Schuhmacher, T. T.; Gillham, R. W.; Reardon, E. J. *Corros. Sci.* **1998**, 40, 371.
- (36) Reardon, E. J. *Environ. Sci. Technol.* **1995**, 29, 2936.
- (37) Balko, B.; Tratnyek, P. G. *J. Phys. Chem. B* **1998**, 102, 1459.
- (38) Puls, R. W.; Blowes, D. W.; Gillham, R. W. *J. Hazard. Mater.* **1999**, 68, 109.
- (39) Blowes, D. W.; Ptacek, C. J.; Benner, S. G.; McRae, C. W. T.; Bennett, T. A.; Puls, R. W. *J. Contaminant Hydrol.* **2000**, 45, 123.

Received for review November 30, 2000. Revised manuscript received June 21, 2001. Accepted July 2, 2001.

ES001923X